This document was prepared in conjunction with work accomplished under Contract No. DE-DE-AC09-76SR00001with the U.S. Department of Energy.

TECHNICAL DIVISION
SAVANNAH RIVER LABORATORY

DPST-77-415
ACC. NO. 109737

DISTRIBUTION

R. Naylor, Wilm.
H. F. Ring
J. F. Proctor -
A. A. Kishbaugh
B. L. Taber
S. Mirshak -
J. A. Porter, SRP
P. R. Moore -
J. H. Hershey
D. B. Jett
J. R. Hilley -
J. L. Womack
R. L. Hooker
B. S. Johnson
I. B. New -
R. F. Mittelburg
C. H. Ice, SRL
J. L. Crandall
S. P. Rideout
D. J. MacIntosh -
A. S. Jennings
M. L. Hyder
R. L. Folger
R. F. Bradley
TIS File

August 9, 1977

M E M O R A N D U M

TO: R. T. HUNTOON

FROM: R. S. ONDREJCIN R.S.O.

PREDICTION OF STRESS CORROSION OF CARBON STEEL BY NUCLEAR PROCESS LIQUID WASTES

INTRODUCTION

At the Savannah River Plant (SRP) separations process wastes are stored in large underground mild steel tanks. The high heat waste (HHW) tanks have volumes of 0.75 to 1.3 million gallons. The primary vessel is contained within a secondary steel pan which is in turn supported by an outer concrete shell.

Some of the primary vessels of these tanks have cracked from nitrate stress corrosion. Other vessels, especially the earlier designs (Types I and II), may still be susceptible to cracking, although in later designs (Type III) the primary vessels were constructed of improved materials, were stress relieved and, therefore, should be more resistant to cracking.

This study was undertaken to identify operating conditions of solution composition and temperature that are conducive to nitrate stress corrosion cracking. The results have provided a technical basis for guiding waste management operations to protect the integrity of tanks used for radioactive waste storage.

The electrochemical behavior of synthetic wastes had previously been shown to be equivalent to that of actual wastes so that laboratory studies with synthetic solutions could be expected to give results that were meaningful to plant operations.[1] However, in previous work, standard stress corrosion specimens did not crack in actual wastes probably because the samples were not sufficiently susceptible to cracking in a reasonable time period.[2] A new experimental method was therefore desired. The method and results from it are described in this report.

SUMMARY

The effect of solution temperature and composition on nitrate stress corrosion cracking of carbon steel was examined by means of a specially developed electrochemical tensile test. Tensile samples were strained to fracture in synthetic waste solutions in an electrochemical cell with the sample as the anode. Surface cracking and severe losses of ductility were observed in samples tested in solutions known to cause nitrate stress corrosion cracking.

The electrochemical tensile test data confirm that A 516-70 steel used in Type III waste tanks is superior to the A 285-B grade used in Type I and II tanks and that the supernates from salt receiver tanks are the least aggressive compositions, while fresh wastes are the most aggressive ones.

Temperature and nitrate concentration were the two solution variables that had the greatest effects on mechanical properties of the steel in a statistically designed experiment. Hydroxide and nitrite ions acted as inhibitors, as shown by a second statistically designed experimental series.

An equation was derived that relates elongation of A 285-B in this test to the combined effect of four variables of the solution: 1) temperature from 50-100°C, 2) NO_3^- from 1.5-5.5M, 3) NO_2^- from 0-3.5M and 4) OH^- from 0-5.0M. The test solutions also contained six ionic constituents, in addition to NO_3^-, NO_2^- and OH^-. Surface cracking was observed in all specimens when total elongation in the test was less than the uniform elongation observed in air (~13%). This value is used as a figure of merit to estimate whether stress corrosion cracking of A 285-B would be a risk if the steel were exposed to equivalent solutions and temperature in service. The 13% limit agrees with results obtained for crack growth in wedge opening loaded specimens tested at 97°C and 5.0M NO_3^- concentration with varying OH^- and NO_2^- concentrations.

The electrochemical tensile test was subsequently used to evaluate the potential of specific waste compositions for producing stress corrosion cracking to assist in waste management operations. For example, conclusions based on such measurements helped determine the advisability of four transfers involving 2.0 million gallons of HHW from H to F Area.

This test was also used as one basis for establishing limits on waste compositions and temperature in Technical Standards for waste storage. The recommended values for waste solutions in the tanks are:

Temperature	70°C max
NO_3^- in liquid phase	5.5M max
$OH^- + NO_2^-$ in liquid phase	
1) For NO_3^- <1.0M	
OH^-	0.01M min (pH - 12)
2) For NO_3^- 1.0 to 3.0M	
OH^-	0.1 x NO_3^-M min
$OH^- + NO_2^-$	0.4 x NO_3^-M min
3) For NO_3^- 3.0 to 5.5M	
OH^-	0.3M min
$OH^- + NO_2^-$	1.2M min

DISCUSSION

Background

At SRP, radioactive wastes are stored in tanks of several different designs. High heat waste (HHW) tanks are double-walled right circular cylinders of welded carbon steel, enclosed in a concrete vault.[3] Three designs have been fabricated: Type I, 0.75 million gallon capacity, are as-welded construction and have twelve internal columns to support the tank roof. Type II, 1.03 million gallon capacity, are also as-welded, but the roof is supported by a single column. Type III, 1.3 million gallon capacity, are stress relieved after welding and also have one central column. The primary steel vessels of the Type I and II tanks are made of ASTM Grade A 285-B steel, while ASTM Grade A 516-70 steel was used for Type III tanks. All tanks used for storing high heat wastes contain cooling coils to extract the heat from radioactive decay; in addition, some have air cooling of the bottom and side walls. The wastes may initially contain radioisotopes that generate up to 0.3 watts/l of heat.

SRP has two separations plants: the F Area plant that uses the Purex process to separate plutonium from uranium metal targets; and the H Area plant that uses the HM process to recover enriched uranium from aluminum-uranium alloy fuel. Both processes include

acid dissolution followed by counter-current solvent extraction. The acidic wastes produced by both plants are made basic by NaOH additions in the separations buildings (221-F and 221-H) before being pumped to one of the tank farms.

The wastes from the two areas are initially of different compositions, e.g., H Area waste contains more NO_3^- and less OH^-. Also, the average $[NO_3^-]/[NO_2^-]$ ratio is ~3 in H Area and ~1 in F; thus, providing less inhibitors in H. As the solutions are aged and evaporated to reduce the liquid volume by crystallization of dissolved salts, the supernates remaining in the two areas tend to approach the same range of compositions[1].

Primary containers in five of the twelve Type I tanks and three of the four Type II tanks have leaked. Stress corrosion cracking was proved to be the cause of leaks in one Type II (16H), and it is assumed to be responsible for the leaks in the other tanks that have leaked, also. Tank 16H leaked so extensively that it was retired from service. Earlier investigations of the leakage attributed the cracking to nitrate stress corrosion, and stress relieving of future tanks was recommended to prevent cracking.[4] Other studies by the Engineering Department recommended use of another steel for future tanks and ASTM A 516-70 was used rather than A 285-B steel.[5] Type III tanks include these features. Although service experience with Type III tanks is limited (five years in one tank), no leaks have been observed to date in contrast to earlier tanks that leaked shortly after being placed in service; one after six months, for example.

The previous studies were generally directed toward improving the metallurgical characteristics of new tanks so that they were more resistant to stress corrosion cracking. The present investigation was directed toward defining the ranges of composition and temperature that will minimize the potential for stress corrosion of the steel, particularly in the Type I and II tanks, which may still be susceptible to damage by stress corrosion.

Development of Electrochemical Tensile Test

Electrochemical Reactions

During corrosion in nitrate solutions, carbon steel is proposed[6] to react anodically by

$$3/4\ Fe + H_2O \rightarrow 1/4\ Fe_3O_4 + 2H^+ + 2e^-. \quad (1)$$

Probably at least two cathodic reactions take place with the resultant being

$$NO_3^- + H_2O + 2e^- \rightarrow NO_2^- + 2OH^-. \quad (2)$$

The H^+ produced in the anodic reaction and the OH^- produced in the cathodic reaction do not react together because the anode and cathode are separated. The anode is at the tip of a crack or the

bottom of a pit, while the cathode may be the walls of the crack or the edge of the pit. As the reactions proceed the anode becomes more acidic and the cathode more basic.

Work at the Naval Research Laboratory (NRL) has shown that in stress corrosion cracking of a number of high strength steels the tip of the crack becomes acidic[7], as inferred from Equation (1). Measurement showed the solutions at the crack tip to have a pH of 3.5 consistently. NRL concluded that the pH was controlled by the hydrolysis of the ferrous ion, i.e., the reaction

$$Fe^{+2} + HOH \rightarrow Fe(OH)^{+} + H^{+} \qquad (3)$$

was controlling. In aqueous solutions the hydrolysis constant for this reaction is $[Fe(OH)^{+}]\,[H^{+}]/[Fe^{+2}] = 1 \times 10^{-7}$. Since $Fe(OH)^{+}$ and H^{+} are equimolar, the numerator becomes $[H^{+}]^2$. Taking the logarithm of both sides results in:

$$-7 = 2\log[H^{+}] - \log[Fe^{+2}] \qquad (4)$$

and at the crack tip:

$$pH = -\log[H^{+}] = 3.5 - 0.5\log[Fe^{+2}] \qquad (5)$$

It has also been shown that in nitrate solutions, the severity of cracking increases according to the cation series $Na^{+}<Ca^{2+}<NH_4^{+}$.[8] In addition to causing more cracking, this series is also one of increasing acidity, which causes the open circuit potential of steel to become more and more anodic.[8] A consequence of the open circuit potential of the steel becoming more anodic is that at a corrosion site either the current density at the anode increases or cathodic reactions are stimulated.

Corrosion, the precursor to cracking, is normally under the control of cathodic reactions in aqueous solutions[9] and is relatively unaffected by minor changes in steel composition. The corrosion rate is influenced by the reduction kinetics and diffusion of reactants to cathodic sites. Nitrate is more easily reduced, as part of the cathodic reaction, as the solution becomes more acidic. In a variety of nitrate solutions cracking is most rapid in the most acidic solutions because 1) they produce the largest anodic open circuit potential, and 2) cathodic reactions are stimulated more. As a result, corrosion is accelerated, forming micropits or intergranular trenches faster, and cracking from local tensile stresses is initiated at the anodic portions of corrosion-produced defects.

Thus, based on electrochemical theory, the best approach to reduce cracking would be to inhibit the cathodic reaction. This could be accomplished by increasing the concentrations of either the NO_2^{-} or OH^{-} or preferably both, as seen in Equation (2).

An accepted theory of crack initiation in mild steel by nitrate solutions involves carbon in the steel.[10] Carbon can be present in solid solution or as Fe_3C in the grain boundaries, it acts as

an efficient cathode with the adjacent metal surface forming the anode of the electrochemical cell. This stimulates anodic dissolution very close to the cathode leading to a micropit or trench, the precursor of a crack.

Anodic dissolution of the grain boundaries can be stimulated by impressing an electrical potential and causing a positive current to flow through a test sample. Current flows (and, therefore, the rate of dissolution of the metal) that can be developed for a given potential are defined by anodic polarization curves. Polarization studies show that in certain solutions where the metal shows an active-passive transition, such as mild steel in some SRP wastes, relatively large increases in current flows can be caused by a small increase in potential. Such potential differences may be caused by precipitates, second phases or elements in solid solutions, such as the carbon described above, resulting in the localized attack required to initiate stress corrosion cracking. Based on these considerations, a tensile test apparatus was devised in which the sample could be strained to failure in a desired test solution while corroding under electrochemical control. Thus, the corrosion effects would be forced to occur, and the stress at corrosion-produced defects would be maximized because the sample is strained continuously. This arrangement would be expected, therefore, to provide the maximum differentiation in the effects of solution variables on the mechanical behavior of the specimen.

Experimental Method

The test equipment is depicted in Figure 1. The threaded portion of the specimen screws into the grips of the tensile test machine. Surrounding the specimen is a platinum counter-electrode (cathode) which is one lead connected to a potentiostat. The cell is connected to a standard calomel reference electrode by a "Teflon"* covered string salt bridge which enters the top of the cell and is positioned within 2 mm of the specimen. The other end of the bridge is immersed in a beaker containing test solution and the reference electrode at room temperature. The reference electrode lead is the second connection to the potentiostat and the lead from the threaded portion of the specimen is the third. An environmental chamber controls the temperature of the test specimen, cell, and solution within $\pm 1°C$. Change in solution concentration by evaporation during testing is prevented by a total reflux condenser connected to the cell.

The current flow between the counter electrode (platinum sheet) and working electrode (tensile specimen) is controlled by the potentiostat to within about 1% of the desired valve. Values of either $0.2 mA/cm^2$ or $0.5 mA/cm^2$ were selected because they represent the range of currents that would be obtained if a 0.01V local potential difference existed above the open circuit potential based on polarization curves for the steel in several actual waste supernates. To attain the desired currents, the potentiostat imposes an equal, but opposite, potential on the counter electrode to produce the desired current flow and polarity on the specimen.

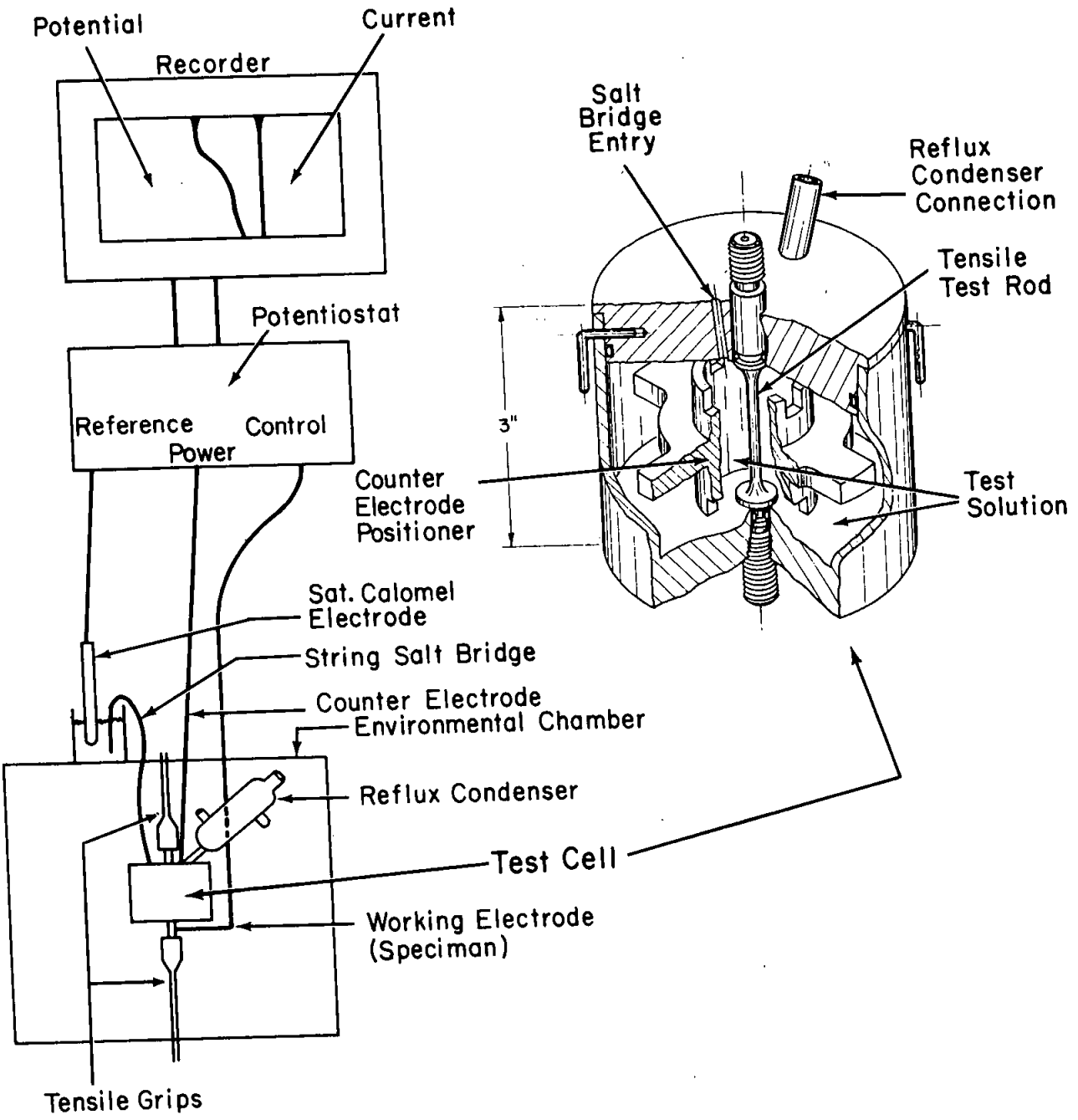

Figure 1. ELECTROCHEMICAL TENSILE TEST EQUIPMENT
(CELL MATERIAL: TEFLON)

Waste Compositions

Typical compositional ranges for HHW and possible effects of the components on corrosion of mild steel are shown in Table I.

Table I

Effects of HHW Constituents on Corrosion

Ion	Concentration Range, M	
NO_3^-	1.6 -4.5	Cracking
NO_2^-	0.0 -3.0	Inhibition (Pitting in very dilute solutions)
OH^-	0.0 -5.0	Inhibition
$Al(OH)_4^-$	0.4 -1.6	Inhibition (OH^- required)
CO_3^{2-}	<0.1 -0.3	Inhibition
SO_4^{3-}	0.02 -0.20	Pitting
PO_4^{3-}	0.01 -0.08	Inhibition
Cl^-	0.005-0.11	Pitting
CrO_4^{2-}	0.001-0.009	Inhibition
F^-	0.001-0.004	Pitting

Synthetic waste solutions were prepared as shown in Table II to correspond to analyses[1] of samples taken either from the waste stored in the tank farm or from fresh waste in the process buildings. Solutions were chosen for wastes in both F and H Areas that would be expected to simulate extremes in aggressiveness (Tanks 1F, 8F and 9F, 14H). The 221-F (Tank 12.1) sample should be typical of fresh wastes generated by the Purex Process at present and the 221-H (Tank 8.4) sample typical of the HM Process. Several special solutions were also made up (H Purex, 11H-13H, 32H).

Table II

Plant Synthetic Test Solutions Based on Analyses

Soln.	Designation	M									µg/ml Hg
		NO_3^-	NO_2^-	OH^-	$Al(OH)_4^-$	CO_3^{2-}	SO_4^{2-}	PO_4^{3-}	Cl^-	CrO_4^{2-}	
F1	Salt	1.6	2.4	6.3	0.8	0.05	0.02	0.08	0.06	0.008	0
F8	Unevap.	1.7	0.5	1.1	0.4	0.05	0.20	0.02	0.03	0.007	40
H9	Salt	1.9	3.2	2.8	1.6	0.10	0.02	0.05	0.03	0.003	130
H14	Unevap.	2.8	2.0	2.5	1.1	0.05	0.04	0.01	0.02	0.003	110
221-F	Purex	2.9	0.0	0.8	0.5	0.0	0.40	0.0	ND	0.01	ND
221-H	HM	4.8	0.0	0.3	1.5	0.0	0.04	0.0	ND	0.00	ND
H	Purex[a]	7.4	0.0	0.5	0.0	0.0	0.28	0.0	0.0	0.0	0.0
H11	Unevap.	3.6	1.2	1.5	0.6	0.01	0.03	0.0	ND	0.004	500
H12	Unevap.	3.0	1.2	1.4	0.4	0.07	0.04	0.0	ND	0.002	200
H13	Unevap.	3.7	0.25	1.4	0.16	0.06	0.10	0.0	ND	0.001	ND
H32	Unevap.	3.3	0.7	1.5	0.7	0.10	0.07	0.0	ND	0.002	260

a. A hypothetical composition calculated from the process flow sheet (DP-990). All other compositions based on chemical analyses of actual solutions, see reference 1.

ND - Not determined.

Materials

Both A 285-B, the material of construction for Tanks 1-8F, 9-16H and A 516-70, the material of construction for Tanks 33-34F, 29-32H, were tested. The microstructures of these hot rolled steels are shown in Figure 2. The much coarser structure and larger amount of ferrite in A 285-B compared to A 516-70 are readily apparent. The composition of the steels and the ASTM specifications for these alloys are shown in Table III.

Table III

	Wt%					UTS	Elong.,
	Mn	Si	C	P	S	kpsi	(%)
A 285-B Actual	0.49	-	0.12	0.010	0.015	55.4	31
ASTM Specification	0.90[a]	-	0.22[a]	0.035[a]	0.045[a]	50-60	25[b]
A 516-70 Actual	1.08	0.24	0.19	0.016	0.022	73.3	21
ASTM Specification	0.80-1.25	0.13-0.33	0.28[a]	0.035[a]	0.040[a]	70-85	17[b]

a. Maximum

b. Minimum

Experimental Results

The response of the two steels in the electrochemical tensile test in the various synthetic solutions relative to the properties measured in air are shown in Table IV.

Table IV

Tensile Properties in
Electrochemical Tensile Test at 100°C and 0.5ma/cm²

	Value in Solution Indicated Relative to Value in Air, %		
A 285-B	Ultimate Strength	Elong.	Reduction in Area
1F	100	100	95
9H	100	72	36
8F	96	50	33
14H	87	38	21
A 516-70			
1F	100	87	88
9H	100	73	71
8F	100	60	68
14H	100	60	68

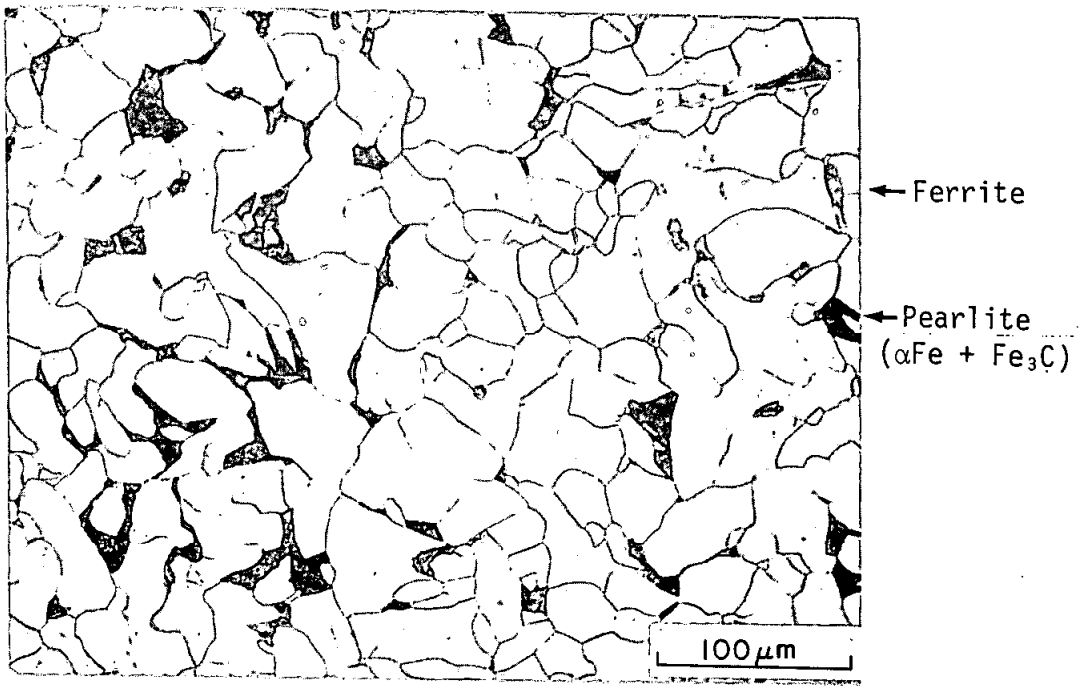

FIGURE 2. Longitudinal Microstructure of A 285-B Carbon Steel

These results show that A 516-70 is generally superior to A 285-B in resisting degradation in these solutions. The strength of A 516-70 was not affected by any of the solutions, and the decrease in ductility is much less than for A 285-B. The data also show that even if no change occurs in strength, ductility values may decrease by as much as 1/3.

The appearance of the A 285-B tensile specimens arranged in order of decreasing ductility from left to right is shown in Figure 3. The highest ductility was shown by samples tested in air and 1F, the sample in 9H was intermediate, while 8F and 14H, solutions representing new waste directly from the process buildings, produced the least ductility. The latter samples had some small cracks along the gage length. Metallographic examination of these cracks (Figure 4) showed them to be typical of nitrate cracking, intergranular with the appearance of loose grains and corrosion produce in the crack.

The test data plotted in Figure 5 also show correlation between ultimate tensile strength and hydroxide concentration, as might be expected from Equation (2) if the corrosion reaction is under cathodic control. These results indicate that attack of A 285-B by H Area wastes aged about one year (11-13H and 32H) would have no more effect on strength than fresh 221-F Purex waste. Fresh 221-H waste proved to be the most aggressive solution encountered in Plant operations. Furthermore, an acidified 8M $NaNO_3$ solution degraded the ultimate strength to about the level of the normal yield strength and produced a fracture with essentially no plastic deformation. Such a solution is strongly aggressive in producing stress corrosion in mild steels.[8]

Fractographs showed greatest damage when the nitrate solutions contained the lowest concentrations of NO_2^- and OH^-. Figure 6 shows that the sample in 221-F Purex cracked along the gage length and failed with almost no reduction in area (total NO_2^- and OH^- was 0.8M). The other two samples (with total NO_2^- and $OH^- \geq 1.6M$).did not crack and showed more ductility with a shear fracture profile. The fracture surfaces were severely corroded; the 221-F Purex sample also showed frequent intergranular separations, and a fracture surface more characteristic of brittle rupture. The other two samples showed dimples resulting from microvoid formation that is typically found in the fracture of a very ductile material.

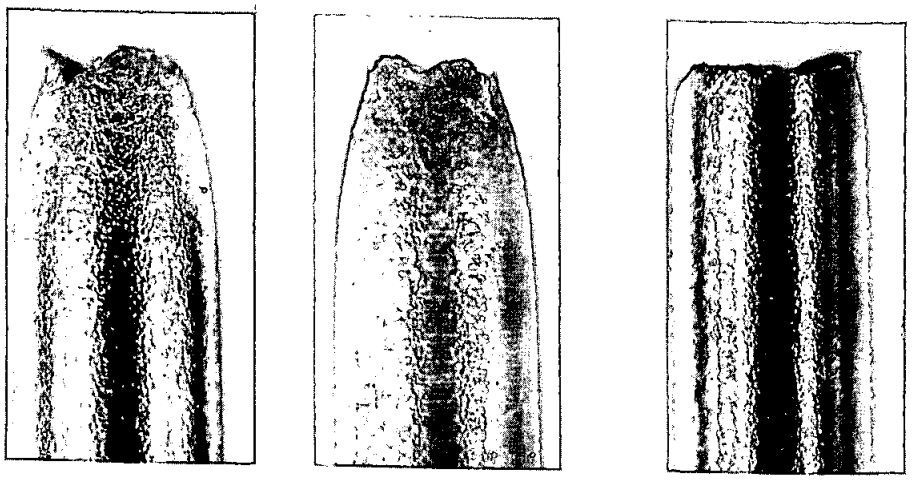

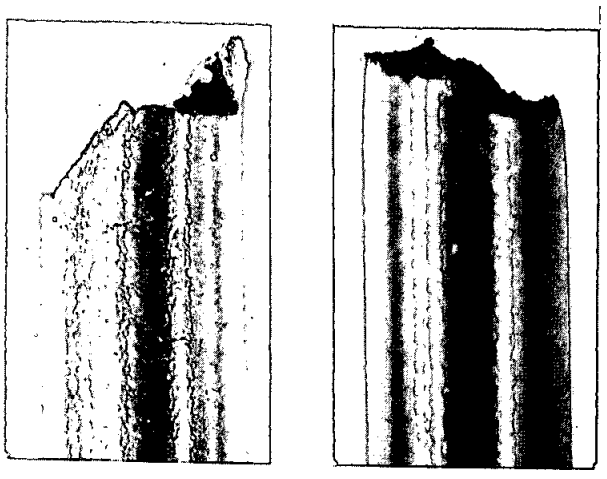

Figure 3. A-285-B TENSILE SPECIMENS TESTED IN VARIOUS MEDIA.

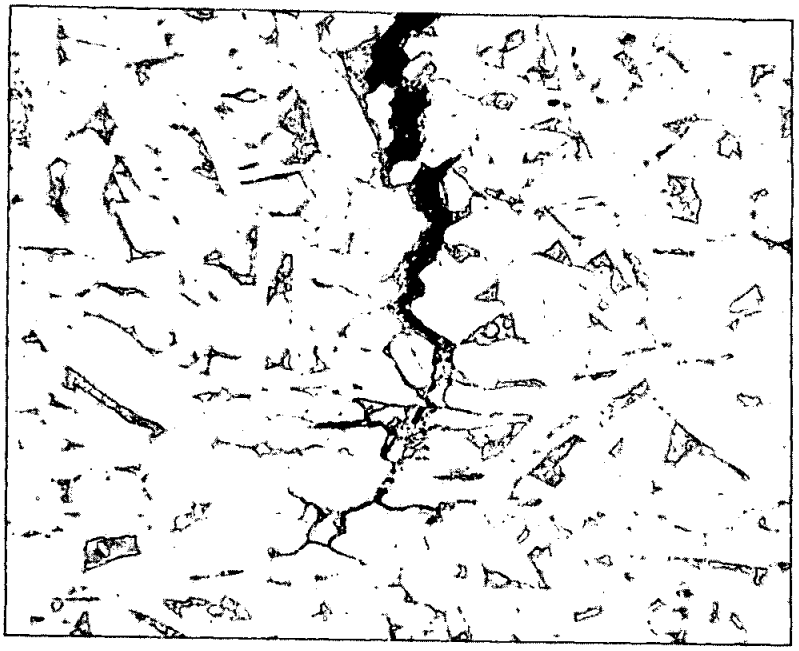

Figure 4. INTERGRANULAR CRACKING OF A-285-B IN CONSTANT CURRENT TENSILE TEST

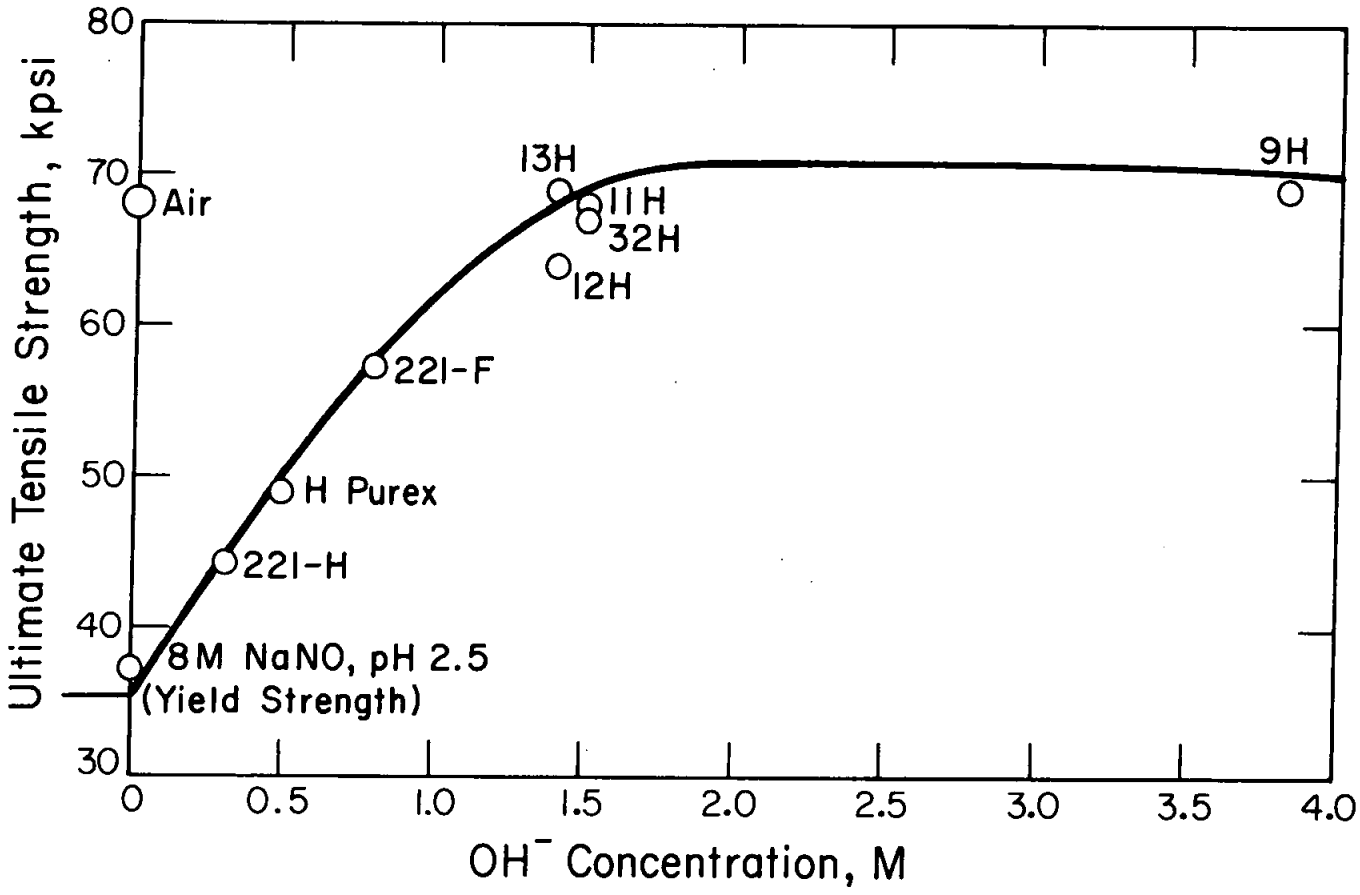

Figure 5. ELECTROCHEMICAL TENSILE TEST, VARIATION OF STRENGTH WITH HYDROXIDE CONCENTRATION OF A 285-B, 100°C, 0.2 ma/cm²

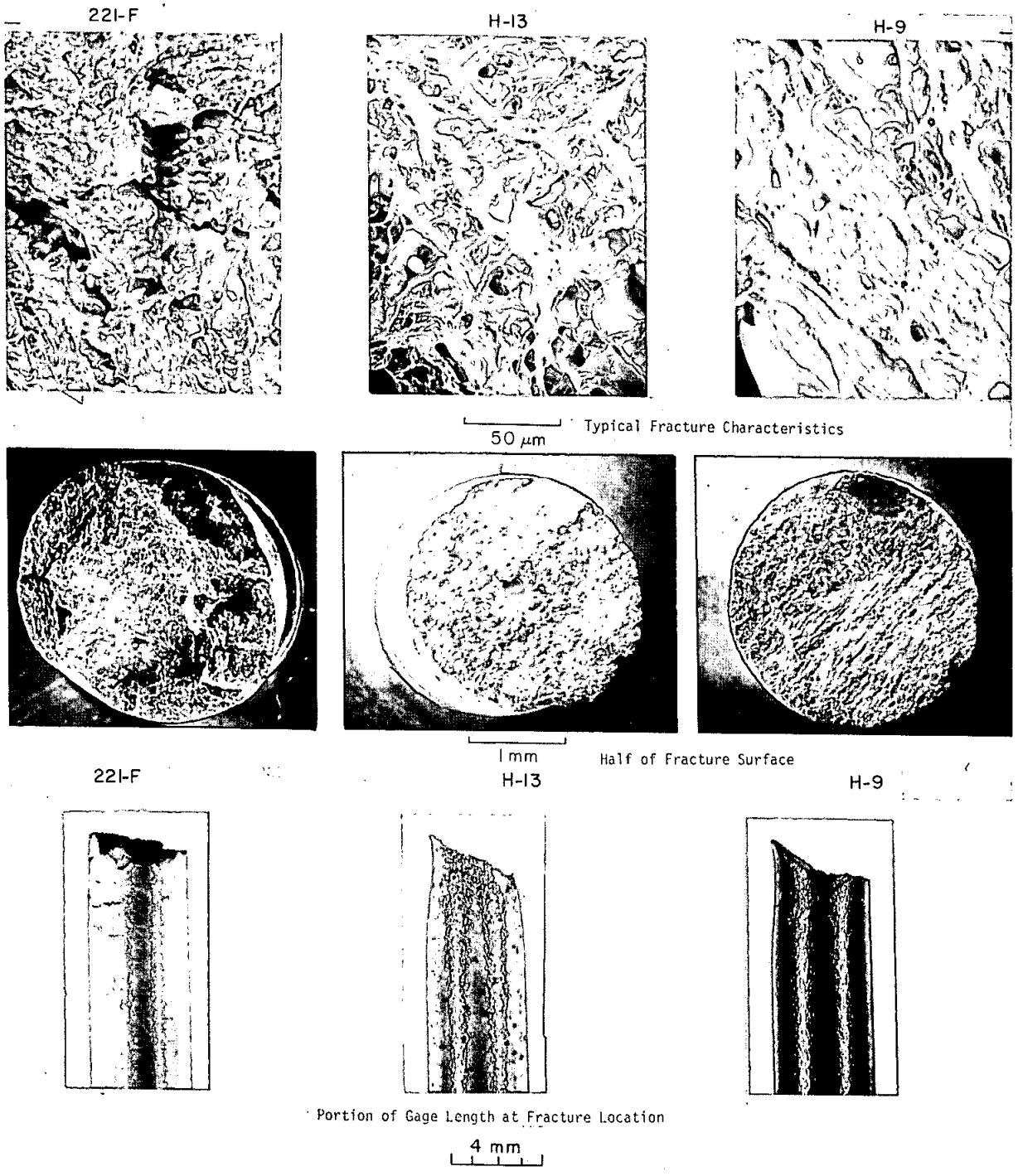

Figure 6. FRACTURE CHARACTERISTICS OF A 285-B in 0.2 ma/cm^2 TENSILE TEST

The above tensile tests were made at 100°C. Less degradation in tensile properties was observed at lower temperatures because of decreased corrosion rates. This is shown for A 285-B in 221-H waste, an aggressive solution, at three different temperatures in Table V.

Table V

Relative Tensile Properties of A 285-B in 221-H Waste at 0.2 ma/cm^2

	Fraction of Values in Air, %		
Temp., °C	Ultimate Strength	Elong.	Reduction In Area
50	100	100	100
75	95	50	70
100	65	30	20

These data indicate that wastes as aggressive as 221-H should be stored at <75°C (preferably <50°C) if the tensile properties are an important factor in nitrate cracking.

Statistical Evaluation of Effects of Variables

Results with simulated wastes showed a pattern of aggressive attack that was consistent with Plant experience:

a) fresh waste at high temperature was most likely to produce SCC
b) fresh H-Area waste was somewhat more aggressive than that in F Area.

Except for OH^-, however, direct correlations of attack with specific values of ionic concentrations could not be developed from the preliminary data. For this reason a detailed statistical evaluation of the effects of the variables was undertaken. Two experimental designs were followed: the Plackett-Burman - to identify the major variables; and the Box-Behnkin - to evaluate the effects of these variables.

Plackett-Burman Series

A Plackett-Burman design[11] was used to identify the major variables. This design is generally used for screening the variable space in selected portions of a 2^n factorial design where one variable is changed at a time with a high and a low value for each. As a screening design, the Plackett-Burman has the advantage that a relatively small number of experiments is required to investigate a large number of independent variables. It has the disadvantage of eliminating interaction effects, such as the effects of inhibitors, and presenting them as an inflation of experimental error.

Because many independent variables can affect the cracking, the Plackett-Burman test series included seven independent variables, temperature and six anionic concentrations. This approach required only 12 experiments rather than 128 for a 2^n factorial with one high and one low value for each independent variable. The variables are shown in Table VI.

Table VI

Plackett-Burman Variables and Constants

Independent Variables			Dependent Variables	Constants[a,b]	
	Low[a]	High[a]			
Temp.(°C)	50	100	UTS	$CO^{2}_{3}^{-}$	0.1
NO_3^-	1.5	5.5	Total Elongation	$SO^{2}_{4}^{-}$	0.1
NO_2^-	0	3.5	Uniform Elongation	$PO^{3}_{4}^{-}$	0.05
$Al(OH)_4^-$	0	1.6	Reduction in Area	$CrO^{2}_{4}^{-}$	0.005
OH^-	0	6.0			
Cl^-	0.005	0.15			
$HHgO_2^-$	0	0.002			

a) All ionic values are M
b) Added to simulate HHW

Four dependent variables, ultimate tensile strength (UTS) and three measures of ductility, were chosen as properties that might be affected by the independent variables. These are shown in Figure 7, a stylized stress-strain curve. The ultimate strength is the point on the curve where uniform elongation ends and necking begins. Total elongation at fracture and uniform elongation provide two measures of ductility; the reduction in cross sectional area that results during necking provides the third.

Analyses of the Plackett-Burman data showed that temperature and NO_3^- concentration stood out above interactions and experimental error in affecting ductility variables. All three ductility variables correlated at the 90% confidence level with the experimental variation in temperature and NO_3^- concentration. In the case of UTS, however, ion interactions apparently caused inflation of experimental error, and no statistically significant correlation to the independent variables was found. From the previous results (Figure 5), the OH^- concentration was believed to be an important interacting ion. Also, equation 2 and electrochemical theory[13,14] would predict both OH^- and NO_2^- to be influential interacting ions. In order to evaluate the correlations between interacting ions and the independent variables, an additional statistically designed experiment was performed as described in the following section.

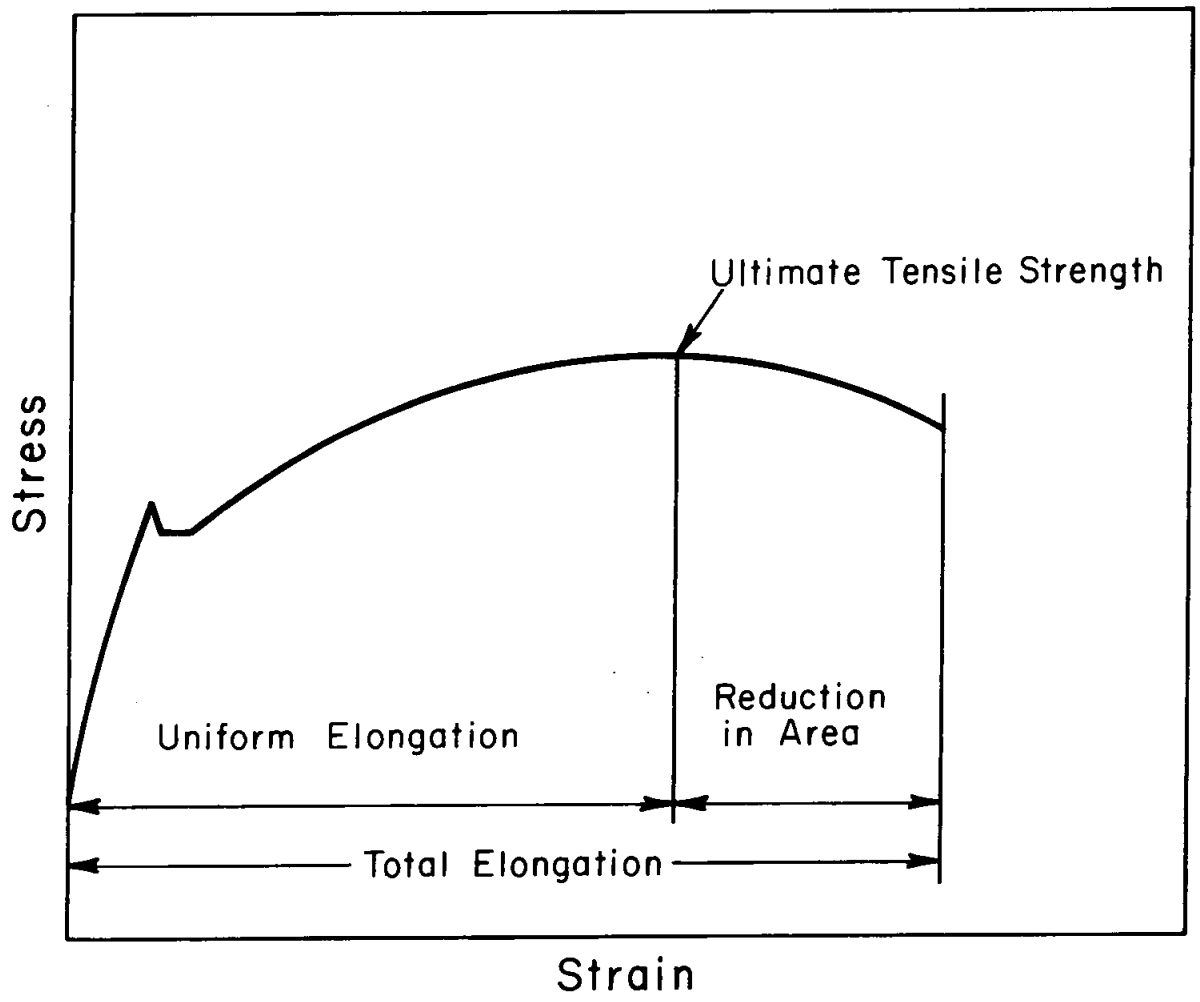

Figure 7. STYLIZED STRESS-STRAIN CURVE.

Box-Behnkin Series

The simultaneous effects of temperature, nitrate, nitrite and hydroxide on strength and ductility of A 285-B were systematically evaluated using a Box-Behnkin series of experiments.[12] A four dimensional computer analysis of these data combined with the Plackett-Burman data resulted in two equations, one for ultimate tensile strength and one for elongation. These equations predict the strength or ductility for any combination of temperature and nitrate, nitrite and hydroxide concentrations within the ranges of 50-100°C, 1.5-5.5M NO_3^-, 0-3.5M NO_2^-, and 0-5.0M OH^-. The predictions can be printed out as contour maps, operating maps, or values for specific combinations of the four independent variables.

In the Box-Behnkin series, other constituents in the waste were held constant. One of these, aluminate, is a major constutuent and is known to have a significant effect on caustic cracking, probably because of the hydroxide required to keep it in solution. However, it apparently has at most a minor effect in nitrate cracking. Of the minor HHW constituents, $SO_4^=$ and Cl^- are often corroding agents and, therefore, could initiate the stress corrosion cracking sequence. Mercury changes the open circuit potential of steel by 0.4-0.5V in the positive direction and could put the steel in the potential range for nitrate cracking. The wastes also contain inhibitors, such as CO_3^{2-}, PO_4^{3-}, and CrO_4^{2-}; some at high enough concentrations to inhibit steel corrosion in water. Therefore, these ions were included in the test solutions at a constant level which simulates the concentrations routinely found in HHW.

A limited series of electrochemical tensile tests was selected based on the Box-Behnkin statistical series. The usual method of varying each factor individually (factorial design) would have required prohibitively extensive testing as seen in Table VII.

Table VII

Factorial and Box-Behnkin Designs

Independent Variables	Number of Experiments: Three Level Factorial	Box-Behnkin Design
3	27	15
4	81	27
5	243	46

The conditions selected for the experimental series are shown in Table VIII.

Table VIII

Box-Behnkin Conditions

Independent Variables	Range	Dependent Variables	Constants[a], M	
Temp.(°C)	50-100	Ultimate Strength	$Al(OH)_4^-$	Sat.0-1.5
NO_3^- (M)	1.5-5.5	Total Elongation	$CO^{2}_3^-$	0.1
NO_2^- (M)	0 - 3.5	Uniform Elongation	$SO^{2}_4^-$	0.1
OH^- (M)	0 - 5.0	Reduction in Area	$PO^{3}_4^-$	0.05
			$CrO^{2}_4^-$	0.005
			$HHgO_2^-$	0.002

a) Added to simulate HHW

Tests at appropriate combinations of the low, mean, and high values of the independent variables were run. The combinations were assigned to each test according to the standard four variable Box-Behnkin design, and the corresponding tensile tests were performed in random order.

For the data reduction, a multiple regression, least squares program was used with the following features: 1) a full quadratic model, 2) an augmented correlation matrix to show correlation among all independent and dependent variables, and 3) analyses of residuals to reject results with large errors. The program also could plot dependent variables against each other to test whether each dependent variable measured the same or different effects. Other output data included equations representing the dependent variables and contour maps of the fitted dependent variables.

To improve the precision of the equations describing the response surfaces, especially in certain sections, the Box-Behnkin data (27 tests) were combined with the Plackett-Burman data (12 tests) and five additional experiments were completed. Only one result of the 44 was rejected based on the computer analysis of residuals; the remaining were used to establish the equations for the response surface.

The resulting experimental design was quite good; the efficiency was 30% (predictions are 30% as precise as the most precise experimental design possible). An actual experimental series cannot usually be designed to exceed 50% efficiency and nonstatistical experimental series with 1-5% efficiency are common.

Cross plots of the four dependent variables showed that only two responses were present, one for UTS and one for ductility (total elongation, uniform elongation or reduction in area). The first equation relates UTS to changes in NO_3^- and OH^- concentration.

The second equation for ductility was similar to the first, but more complex. Ductility correlated with temperature, nitrate, nitrite and hydroxide, with the nitrate effect depending on temperature as well as on nitrite concentration.

The ductility response was chosen as the more important because stress corrosion is a phenomenon in which normally ductile material behaves in a brittle (less ductile) manner. The equation was developed specifically for total elongation because this is the simplest ductility property to measure in a tensile test. The equation is given in Table IX. The equation is long (33 coefficients), but relatively simple in that it only has linear, cross-product and quadratic terms of the four independent variables.

One way to use the equation is to generate families of curves representative of concentrations or temperatures of interest. One such family is illustrated in Figure 8, in which conditions are similar to those that might be expected for fresh HHW; temperature is high, 100°C, and nitrite is low. Analyses have shown <0.05M nitrite to be present in Purex and HM wastes directly from the 221 Buildings. Elongation is plotted against hydroxide concentration for several concentrations of nitrate. The line at 13% elongation separates samples that always cracked during the test from samples that generally did not show surface cracking. (See also the discussion below).

Data calculated from the equation can also be illustrated as a contour map. Any two of the four independent variables are held constant on a given map with the other two variables plotted against each other. The contour lines separate selected ranges of the dependent variable. A series of maps may be printed with incremental changes in either of the two independent variables not plotted, and the contour lines gradually shift. Figure 9 shows one such map in which hydroxide is plotted against nitrate at constant temperature and nitrite concentration. The contours indicate conditions that produce constant elongations. Figure 10 gives a series of sections showing the shift with temperature of the contours delineating 13% elongation.

General contour maps are usually too complex for operation of a process. Normally operating limits are chosen, and printouts made that illustrate "operate-do not operate" areas on a series of maps. Typical examples are shown in Figure 11 and 12. Most fresh wastes fall in the lower left-hand quadrants of these maps.

The absence of any contours in the map for 50°C, even at 0.0M NO_2^- indicates that below this temperature, wastes within the compositions tested should not initiate the stress corrosion sequence, as defined by the electrochemical tensile test. Once initiated, however, cracks might propagate in this region.

TABLE IX

$$\% \text{ Elongation} = .9956366+01 - .7667758-02\,X_1 + .1007542-01\,(X_1)^2 + .3298862+00\,X_2 - .6213454-01\,(X_2)^2 - .8550595-01\,X_3 + .1072422+01\,(X_3)^2 + .3750973-01\,X_4 + .1164742+01\,(X_4)^2 + .8778023-03\,X_1X_2 + .3684767-02\,X_1(X_2)^2 - .6804358-03\,(X_1)^2X_2 + .2349247-03\,(X_1)^2(X_2)^2 + .1702175-01\,X_1X_3 - .1927237-01\,X_1(X_3)^2 - .1296127-02\,(X_1)^2X_3 - .1996026-02\,(X_1)^2(X_3)^2 + .9771332-02\,X_1X_4 - .2234101-02\,X_1(X_4)^2 - .8668608-04\,(X_1)^2X_4 - .1516368-02\,(X_1)^2(X_4)^2 + .1733371+00\,X_2X_3 - .1255511+00\,X_2(X_3)^2 + .1488442+00\,(X_2)^2X_3 + .2951515+00\,(X_2)^2(X_3)^2 + .8594171-01\,X_2X_4 - .3940304-01\,X_2(X_4)^2 + .7889912-01\,(X_2)^2X_4 + .3251255-01\,(X_2)^2(X_4)^2 - .4380164-01\,X_3X_4 + .1005124+00\,X_3(X_4)^2 - .5484608-02\,(X_3)^2X_4 - .2021886+00\,(X_3)^2(X_4)^2$$

where

X_1 = Temp.°C - 75

X_2 = M NO_3^- - 3.5

X_3 = M NO_2^- - 1.75

X_4 = M OH^- - 2.5

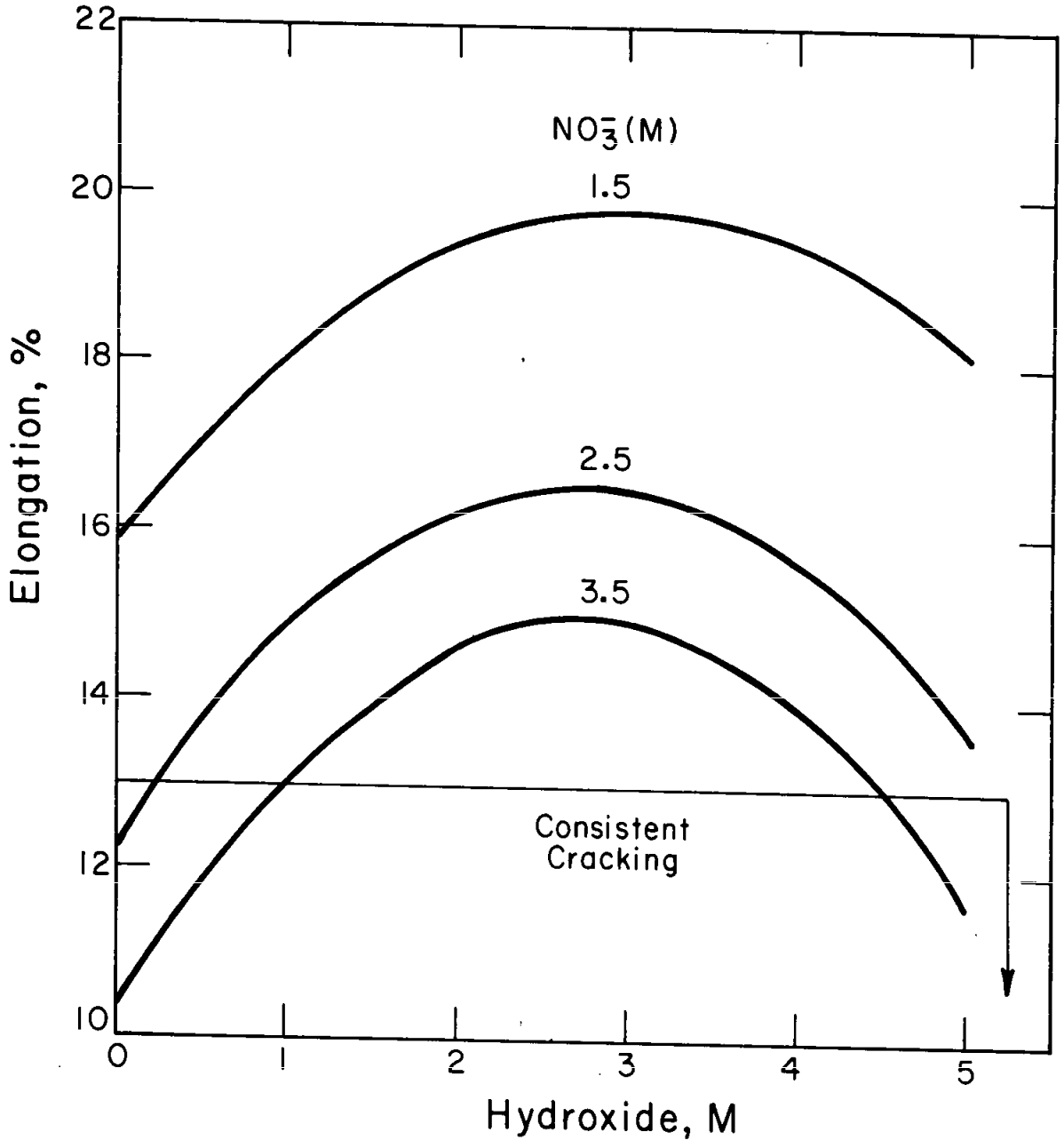

Figure 8. MILD STEEL (A-285-B) ELONGATION VS. HYDROXIDE CONCENTRATIONS IN HHW, 100°C, 0.0M NITRITE

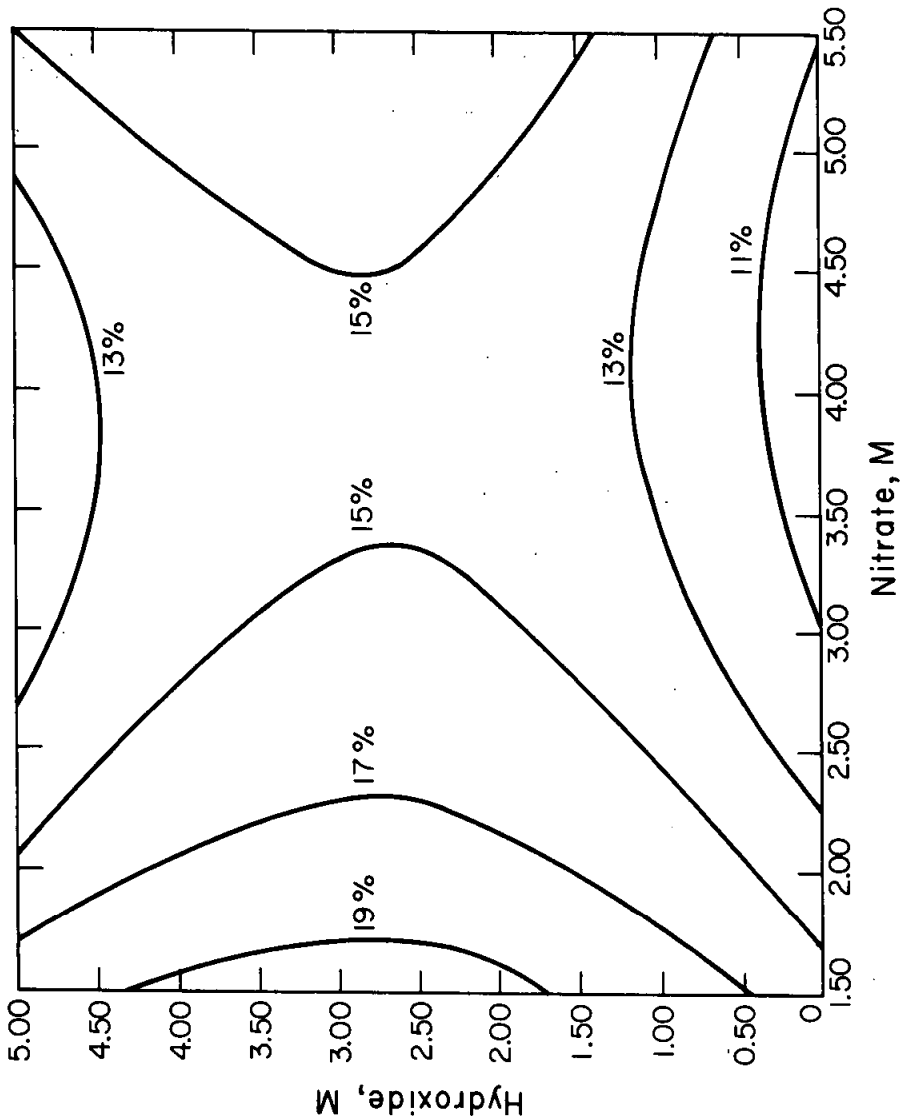

Figure 9. CONTOUR MAP OF A-285-B ELONGATION IN ELECTROCHEMICAL TENSILE TEST, 100°C, 0.OM NITRITE

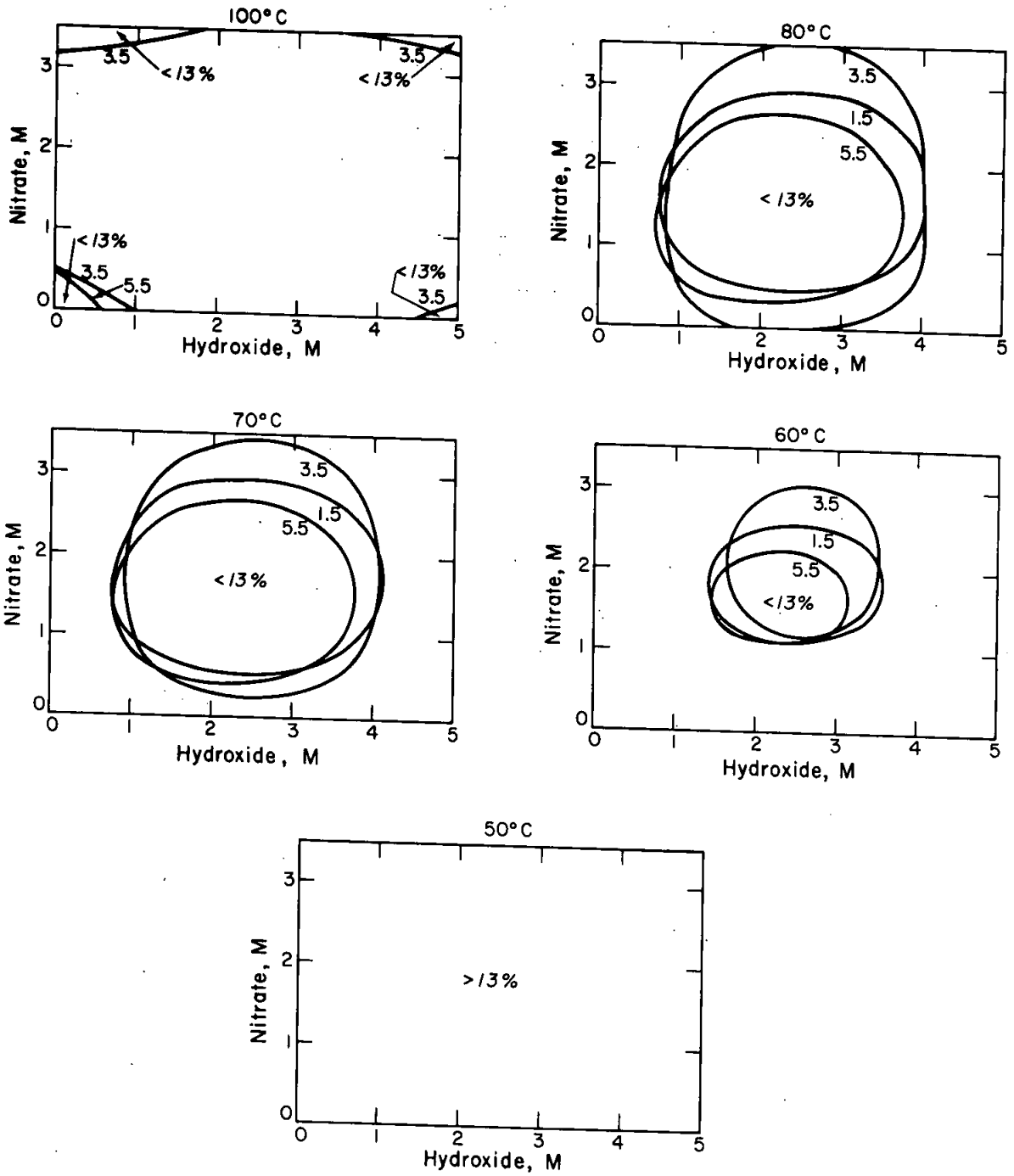

Figure 10. CONTOURS OF 13% ELONGATION AT VARIOUS TEMPERATURES

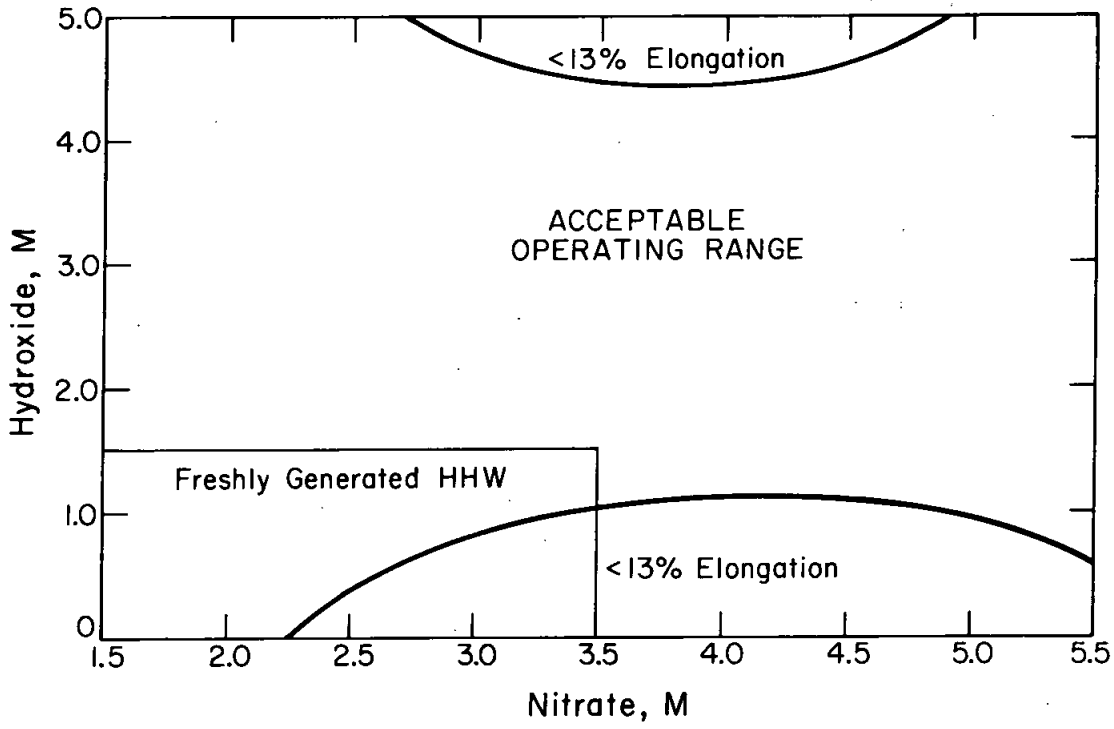

Figure 11. OPERATIONAL CONTOUR MAP, 100°C, 0.0M NITRITE

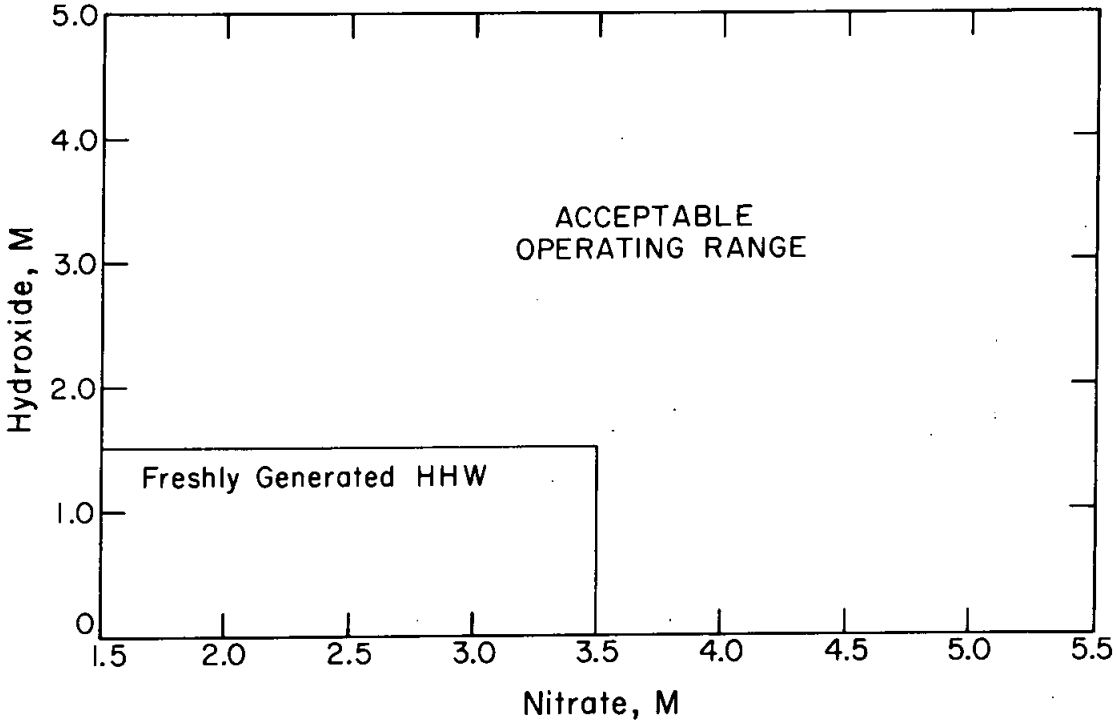

Figure 12. OPERATIONAL CONTOUR MAP, 50°C, 0.0M NITRITE

The limit of 13% total elongation was selected as a figure of merit in these contour maps for three reasons. First, the samples from the Plackett-Burman and Box-Behnkin series were examined. At 13% or less total elongation, A 285-B samples always showed surface cracks along the gage length. At greater elongations such cracking was unusual and always minor if observed. Second, evaluation of tensile test data in air at elevated temperature showed that the limit of uniform elongation was about 13%. This is the point of maximum load and the point at which stresses in a tensile specimen change from biaxial to triaxial. Triaxial stresses are generally considered to be more effective in crack initiation of polycrystalline materials. Finally, the 13% limit was consistent with results of tests using a fracture mechanics approach to evaluate crack growth[15]. These tests used wedge-opening-loaded specimens at 97°C, 5.0M NO_3^- in the ranges of 0-1.5M NO_2^- and 0-1.5M OH^-.

A region in which the indicated elongation is less than 13% exists in the center of the variable space between about 57° and 94°C, as shown in Figure 13. This region is an irregular volume centered at approximately 2M NO_2^- and 2.5M OH^-; the volume enclosed is maximum at about 3.5M NO_3^-. The low value of elongation in this region is largely influenced by the single point determined by triplicate tests that gave a low elongation at 75°C and 3.5M NO_3^-, 1.75M NO_2^- and 2.5M OH^-. According to the statistical tests included in the Box-Behnkin analysis, this result was a valid test. (As indicated above, one other result among the 44 tests was excluded from the analysis based on these tests.)

Additional tests are in progress to confirm that this region does exist, to establish its boundaries more precisely, and to determine the phenomena that cause it.

It may be due to an effect of temperature on the solubilities of O_2 perhaps combined with some other species in the solution. Corrosion of mild steel has been observed to be maximum at 80°C, decreasing at both lower and higher temperature[16]. The higher temperatures decrease O_2 solubility enough to decrease the corrosion rate, while at lower temperatures the corrosion rate also decreases because of a decrease in reaction rates. Smialowski and Ostrowska[17] contend that O_2 is of great importance in assisting the nitrate cracking mechanism, although Herzog and Portevin[18] claim it is without effect. The differences in interpretation could be due to temperature and its effect on O_2 solubility.

The presence of this region could be significant to waste operations, because two tanks, 11H and 12H, have waste compositions that could lie within the enclosed volume based on the most recent analyses of their contents. As shown in Figure 14 these solutions would produce an elongation of less than 13% at temperatures >65°C. However, the actual solution temperatures are 37°C for 11H and 38°C for 12H so that the tanks will meet the 13% elongation criterion throughout the period of initial aging of the waste. When the contents are evaporated to reduce solution volume, the compositions will shift as shown and remain in a region with greater than 13% elongation.

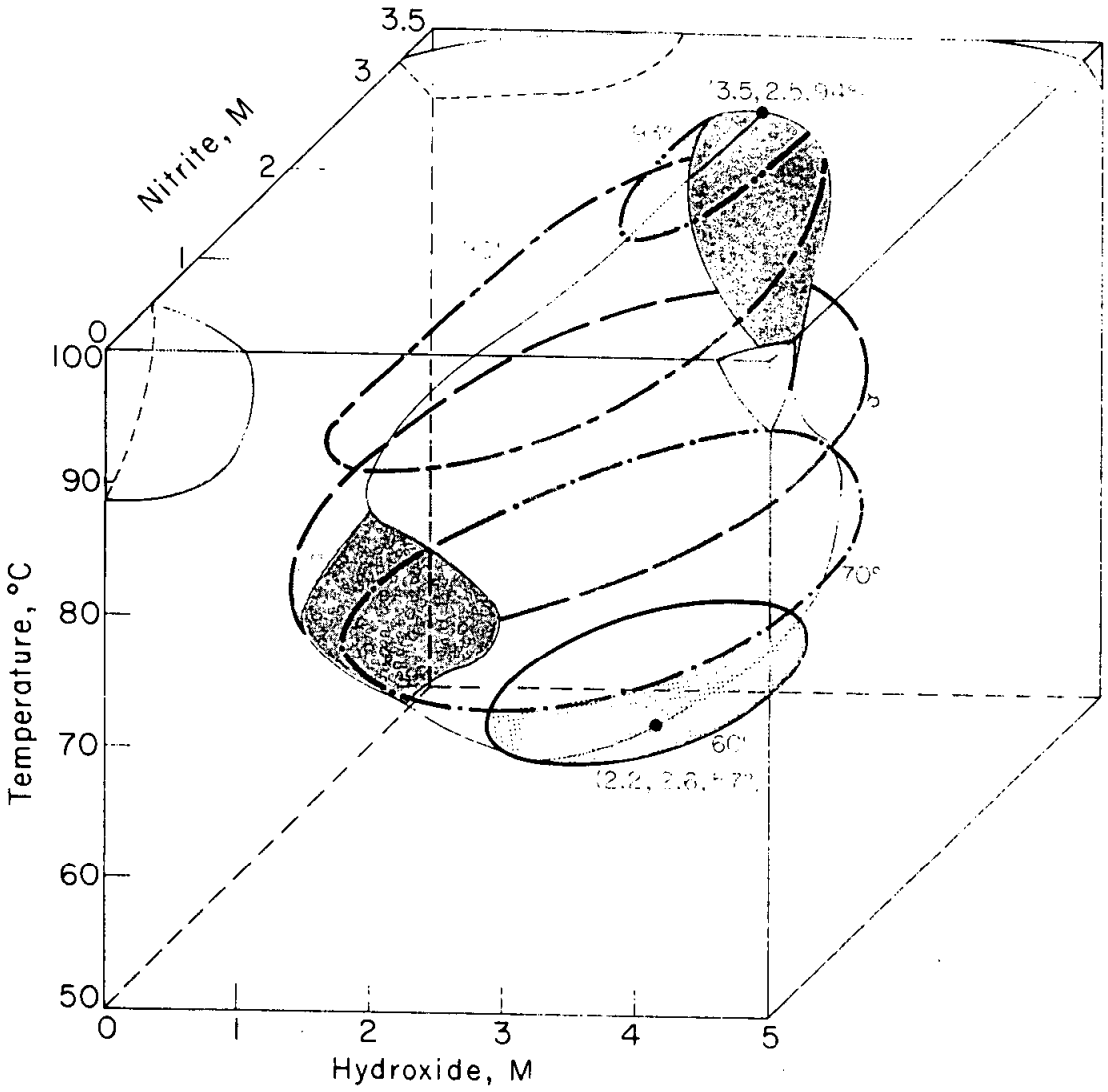

Figure 13. EQUATION DEPICTED AT 13% ELONGATION AND 3.5M NITRATE

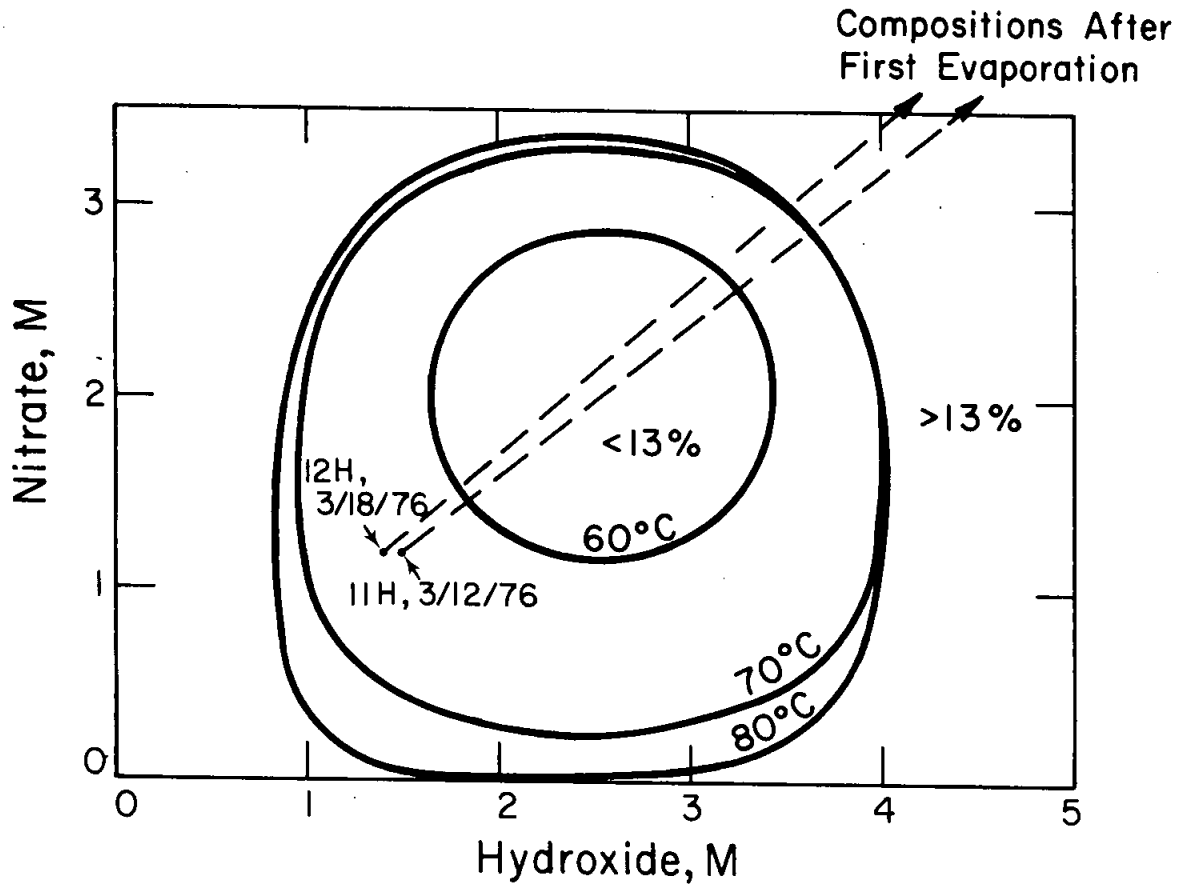

WASTE COMPOSITIONS (PRINCIPAL ANIONS ONLY) ARE GIVEN BELOW:

Tank	Sample Data	Concentration, - M NO^-_3	OH^-	NO^-_2	$Al(OH)^-_4$
11H	3/12/76	4.0	1.5	1.2	0.6
12H	3/18/76	2.8	1.4	1.2	0.4

FIGURE 14. WASTE COMPOSITIONS IN TANKS 11H AND 12H COMPARED TO 13% ELONGATION - CONTOURS AT 4.0 M NO^-_3

Applications to Plant Operations

Interarea Transfers

The transfer of wastes between areas is desirable to optimize HHW evaporator operations and waste tank utilization. Prior to these studies the transfer of waste from H to F Area was considered to be inadvisable. H Area wastes were generally believed to be more aggressive to Type I and II tanks (not stress relieved) than F Area wastes, as evidenced by a much higher incidence of stress corrosion cracking in H Area.

A test sequence was developed to examine this question. The sequence included chemical analyses of the wastes, potentiodynamic polarization curves on the actual and synthetic wastes prepared on the basis of the chemical analyses, electrochemically controlled tensile tests and wedge-opening loaded tests in synthetic waste solutions. Since the polarization curves were essentially identical, the steel would be expected to react the same way in synthetics and actual wastes. Electrochemically controlled tests determined susceptibility to crack initiation, wedge-opening loaded specimens determined susceptibility to crack propagation.

For the electrochemical tensile tests, the elongation values calculated from the ductility equation, Table IX, are compared with measured values in Table X.

TABLE X

Results of Electrochemical Tensile Tests at 100°C

	Solution Composition, M			Total Elongation, %		
Tank	NO_3^-	NO_2^-	OH^-	Predicted	Measured[a]	Vol. from H to F Area Transferred, gal.
11H	3.6	1.2	1.5	16	17	413,000
12H	3.0	1.2	1.4	16	15	Deferred[b]
13H	3.7	0.26	1.4	14	16	496,000
32H	3.3	0.70	1.5	16	17	1,069,000

a. Average of 2 values.

b. Transferred within H-Area.

The measured values were above the 13% elongation criterion. The average difference between the predicted and measured values for the four tests is 8% or about the error expected for a tensile test in air. The data provided a basis for approving the

transfer of 2.0 million gallons of HHW from H to F Areas, as indicated in the table.

Recommended Limits for Liquid Wastes

The limits shown in Table XI have been recommended for the Technical Standards for The Waste Tank Farm.[19] The limits for high nitrate contents are based on the results of the electrochemical tensile test, which emphasize conditions for crack initiation, as well as results from studies using wedge-opening-loaded specimens. Such specimens were used to evaluate conditions which cause crack propagation. Data for both methods are summarized in Figure 15. Note that good agreement exists for the two approaches in that compositions that cause cracks to form also cause them to grow.

The required minimum OH^- and NO_2^- concentrations are reduced at lower NO_3^- contents in keeping with the result from the present study, Figure 8, for example. Below 1M NO_3^- nitrate stress cracking does not occur[10]; the minimum OH^- content of 0.01M is specified to prevent pitting attack.

The maximum temperature of 70°C is the lowest value that can normally be maintained in the tanks during storage of fresh separations wastes because of their relatively high heat generation. Low temperatures are generally desirable because they reduce corrosion reaction rates. After evaporation the wastes are returned from the evaporator at nearly the boiling point. Since the concentrations of OH^- and NO_2^- are then quite high, 2.5 to 3.5M for NO_2^-, no corrosion damage should result because of the higher temperatures.

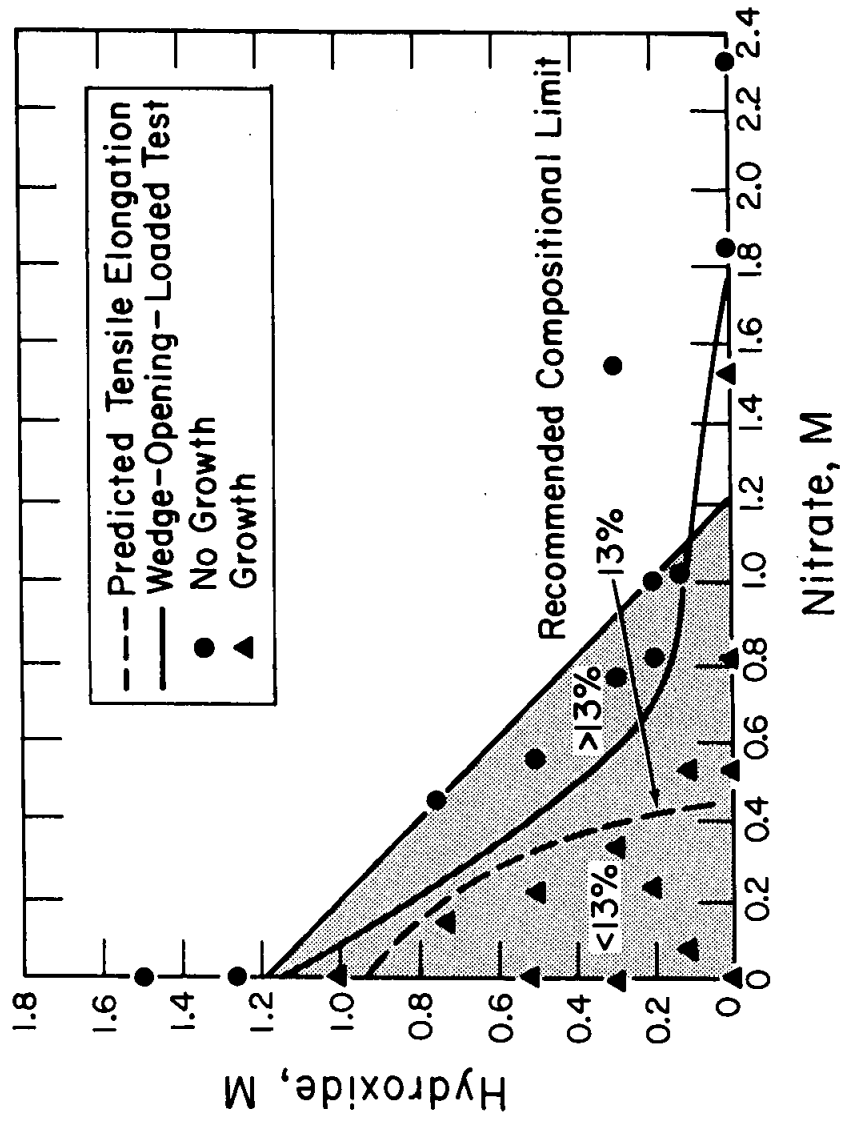

Figure 15. COMPARISON OF ELECTROCHEMICAL TENSILE TEST WITH WEDGE-OPENING-LOADED SPECIMENS IN 5M $NaNO_3$ AT 97°C.

TABLE XI

Recommended Limits for Liquid Wastes

	Min	Max
NO_3^- in liquid phase of concentrated waste	-	5.5M
$OH^- + NO_2^-$ in liquid phase of concentrated waste		
For NO_3^- 3.0 to 5.5		
OH^-	0.3M	-
$OH^- + NO_2^-$	1.2M	-
For NO_3^- 1.0 to 3.0		
OH^-	0.1 x NO_3^-M	-
$OH^- + NO_2^-$	0.4 x NO_3^-M	
For NO_3^- <1.0		
OH^-	0.01M (pH = 12)	-
Temperature of liquid phase		
fresh waste solutions	-	70°C
concentrated wastes		<boiling point

REFERENCES

1. R. S. Ondrejcin. Chemical Compositions of Supernates Stored in SRP High Activity Waste Tanks DP-1347, E. I. du Pont de Nemours & Co., August 1974.

2. Memorandum, "Corrosion Tests, Building 241-F Waste Storage Tank Number 5" to C. Schwab from F. T. Wyman, June 8, 1960.

3. Plan for the Management of Radioactive Waste, Savannah River Plant, SRO-TWN-75-1, E. I. du Pont de Nemours & Co., July 1975.

4. Holzworth, M. L. et. al. "How to Prevent Stress-Corrosion Cracking of Radioactive Waste Storage Tanks", Materials Protection 7, 36-38 (1968).

5. Review of Waste Tank Designs, Savannah River Plant, DPE-2268, Vol. I, August 1963.

6. Hoar, T. P. and J. R. Galvele. "Anodic Behavior of Mild Steel During Yielding in Nitrate Solutions", Corrosion Science 10, 211 (1970).

7. Sandoz, G., Fujii, C. T. and B. F. Brown. Solution Chemistry Within Stress-Corrosion Cracks in Alloy Steels, Corr. Sci. 10, 839 (1970).

8. Parkins, R. N. and R. Usher. The Effect of Nitrate Solutions in Producing Stress-Corrosion Cracking in Mild Steel, First International Congress on Metallic Corrosion, p. 289, Butterworths, London (1962).

9. Legault, R. A., Mori, S. and H. P. Leckie. "An Electrochemical Statistical Study of the Effect of Chemical Environment on the Corrosion Behavior of Mild Steel", Corrosion 6, 121 (June 1970).

10. R. N. Parkins. "Stress Corrosion Cracking of Low Carbon Steels", Proceedings of Conference - Fundamental Aspects of Stress Corrosion Cracking - Sept. 11-15, 1967. National Assoc. of Corr. Eng., Houston, TX, p. 361-373 (1969).

11. Plackett, R. L. and J. P. Burman, "The Design of Optimum Multifactorial Experiments", Biometrica 33, 305-329 (1946).

12. G. E. P. Box and D. W. Behnkin. "Some New Three Level Designs for the Study of Quantitative Variables", Technometrics 2, 455-475 (1960).

13. Parkins, R. N. Stress Corrosion "Cracking of Low Carbon Steels", Fundamental Aspects of Stress Corrosion Cracking, National Association of Corrosion Engineers, Houston, Texas (1969).

14. Smialowski, M. Discussion p. 295, First International Congress on Metallic Corrosion, Butterworths and Co. (1961).

15. Donovan, J. A. "Inhibition of Nitrate Stress Corrosion Cracking of Mild Steel in Nuclear Process Wastes", American Nuclear Society Meeting, June 8-13, 1975.

16. Uhlig, H. H. "Corrosion and Corrosion Control", 2nd ed., John Wiley & Sons, New York, NY (1971).

17. Smialowski, M. and T. Ostrowska, Corr. et Anticorr (March 1957).

18. Herzog, E. and M. Portevin, Metaux et Corrosion 24, 40 (1949).

19. S. P. Rideout to J. R. Hilley. "Revisions to Technical Standards For the Waste Tank Farm - DPST-75-48-29 Rev. 2", October 26, 1976.